NON-LINEARITIES AND RESONANCES

E. Wilson
CERN, Geneva, Switzerland

1. INTRODUCTION

The first step in designing an accelerator or storage ring is to choose an optimum pattern of focusing and bending magnets, the lattice. At this stage, non-linearities in the guide field are ignored. It is assumed that the bending magnets are identical and have a pure dipole field. Gradient magnets or quadrupoles have radial field shapes which have a constant slope, unperturbed by higher-order multipole terms.

Before going too far in fixing parameters, the practical difficulties in designing the magnets must be considered and the tolerances which can be reasonably written into the engineering specification determined. Estimates must be made of the non-linear departures from pure dipole or gradient field shape, and of the statistical fluctuation of these errors around the ring at each field level.

We must take into consideration that the remanent field of a magnet may have quite a different shape from that defined by the pole geometry; that steel properties may vary during the production of laminations; that eddy currents in vacuum chamber and coils may perturb the linear field shape. Mechanical tolerances must ensure that asymmetries do not creep in. At high field the linearity may deteriorate owing to saturation and variations in packing factor can become important. Superconducting magnets will have strong error fields due to persistent currents in their coils.

When these effects have been reviewed, tolerances and assembly errors may have to be revised and measures taken to mix or match batches of laminations with different steel properties or coils made from different batches of superconductor. It may be necessary to place magnets in a particular order in the ring in the light of production measurements of field uniformity or to shim some magnets at the edge of the statistical distribution. Even when all these precautions have been taken, non-linear errors may remain whose effect it is simpler to compensate with auxiliary multipole magnets.

Apart from the obvious need to minimize closed orbit distortion, these measures must be taken to reduce the influence of non-linear resonances on the beam. A glance at the working diagram (Fig. 1) shows why this is so. The Q_H, Q_V plot is traversed by a mesh of non-linear resonance lines or stopbands of first, second, third, and fourth order. The order, n, determines the spacing in the Q diagram; third-order stopbands, for instance, converge on a point which occurs at every 1/3 integer Q-value (including the integer itself). The order, n, is related to the order of the multipole which drives the resonance. For example, fourth-order resonances are driven by multipoles with $2n$ poles, i.e. octupoles. Multipoles can drive resonances of lower-order; octupoles drive fourth- and second-order; sextupoles third- and first-order, etc., but here we simply consider the highest order driven.

The non-linear resonances are those of third-order and above, driven by non-linear multipoles. Their strength is amplitude-dependent so that they become more important as we seek to use more and more of the machine aperture. Theory used to discount resonances of fifth- and higher-order as harmless (self-stabilized), but experience in the ISR, FNAL and SPS suggests this is not to be relied upon when we want beams to be stored for more than a second or so.

Each resonance line is driven by a particular pattern of multipole field error which can be present in the guide field. The lines have a finite width depending directly on the strength of the

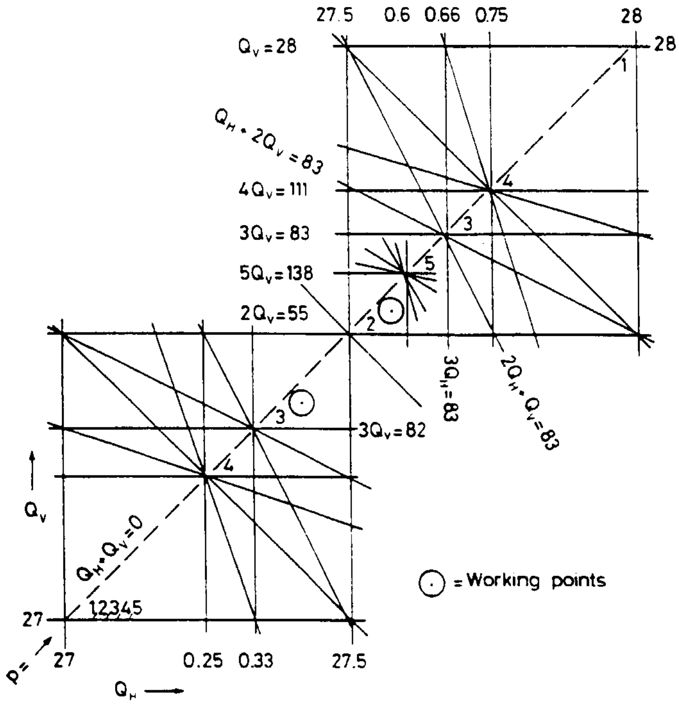

Fig. 1 Working diagram or Q_H, Q_V plot showing the non-linear resonances in the operating region of the CERN SPS

error. In the case of those driven by non-linear fields, the width increases as we seek to exploit a larger fraction of the magnet aperture. We must ensure that the errors are small enough to leave some clear space between the stopbands to tune the machine, otherwise particles will fall within the stopbands and be rapidly ejected before they have even been accelerated. In general, the line width is influenced by the random fluctuations in multipole error around the ring rather than the mean multipole strength.

Systematic or average non-linear field errors also make life difficult. They cause Q to be different for the different particles in the beam depending on their betatron amplitude or momentum defect. Such a Q-spread implies that the beam will need a large resonance-free window in the Q diagram. In the case of the large machines, SPS, LEP, HERA, etc., the window would be larger than the half integer square itself if we did not balance out the average multipole component in the ring by powering correction magnets.

Paradoxically, when a "pure" machine has been designed and built, there is often a need to impose a controlled amount of non-linearity to correct the momentum dependence of Q or to introduce a Q-spread among the protons to prevent a high intensity instability. Sextupole and octupole magnets may have to be installed to this end and techniques studied which will enable the control room staff to find the correct settings for these trim magnets once the machine works.

Yet another set of multipole magnets is often required in a pulsed synchrotron to deliberately excite non-linear betatron resonances and extract the beam in a long slow spill.

With modern computer control, the correction of closed orbit distortion due to linear field errors has become a routine matter and, particularly in large accelerators, most of the emphasis has shifted to calculation and elimination of the non-linear effects which prove to be of considerable importance in the running-in of FNAL and the SPS. In this talk I hope to outline sufficient of the physics and mathematics of non-linearities to introduce the reader to this important aspect of accelerator theory.

2. MULTIPOLE FIELDS

Before we come to discuss the non-linear terms in the dynamics, we shall need to describe the field errors which drive them. The magnetic *vector potential* of a magnet with $2n$ poles in Cartesian coordinates is:

$$A = \sum_n A_n f_n(x,z) \ , \tag{1}$$

where f_n is a homogeneous function in x and z of order n.

Table 1
Cartesian solutions of magnetic vector potential

Multipole	n	Regular f_n	Skew f_n
Quadrupole	2	$x^2 - z^2$	$2xz$
Sextupole	3	$x^3 - 3xz^2$	$3x^2z - z^3$
Octupole	4	$x^4 - 6x^2z^2 + z^4$	$4x^3z - 4xz^3$
Decapole	5	$x^5 - 10x^3z^2 + 5xz^4$	$5x^4z - 10x^2z^3 + z^5$

Table 1 gives $f_n(x,z)$ for low-order multipoles, both regular and skew. Figure 2 shows the distinction. We can obtain the function for other multipoles from the binomial expansion of

$$f_n(x,z) = (x + iz)^n \ . \tag{2}$$

The real terms correspond to regular multipoles, the imaginary ones to skew multipoles.

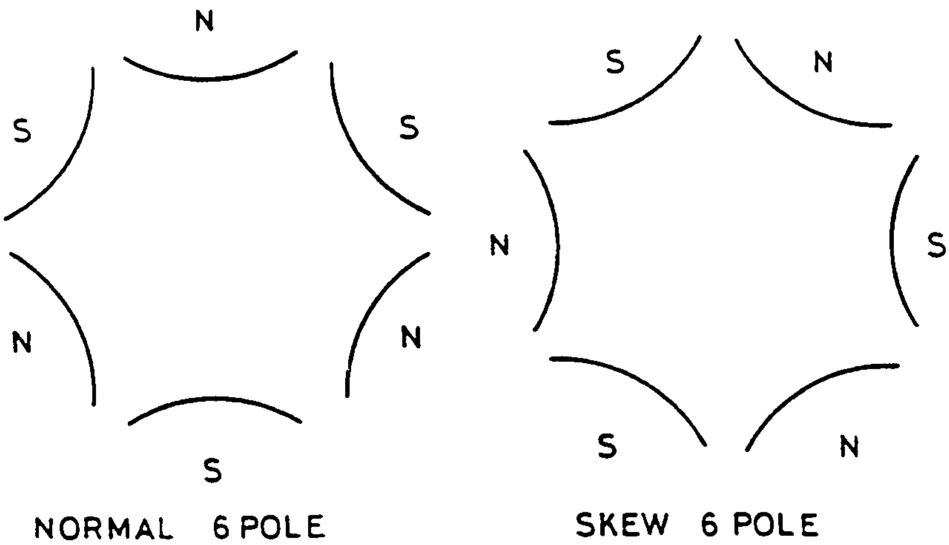

Fig. 2 Pole configurations for a regular sextupole and a skew sextupole

For numerical calculations it is useful again to relate A_n and field, remembering that for regular magnets:

$$B_z(z=0) = \frac{\partial A_s}{\partial x} = \sum_{n=1}^{\infty} nA_n x^{(n-1)} = \sum_{n=1}^{\infty} \frac{1}{(n-1)!} \left(\frac{d^{(n-1)} B_z}{dx^{(n-1)}} \right)_0 x^{n-1} \tag{3}$$

so that

$$A_n = \frac{1}{n!}\left(\frac{d^{(n-1)}B_z}{dx^{(n-1)}}\right)_0 \quad . \tag{4}$$

As a practical example of how one may identify the multipole components of a magnet by inspecting its symmetry, we digress a little to discuss the sextupole errors in the main dipoles of a large synchrotron.

Let us look at a simple dipole (Fig. 3). It is symmetric about the vertical axis and its field distribution will contain mainly even exponents of x, corresponding to odd n values: dipole, sextupole, decapole, etc. We can see, too, that cutting off the poles at a finite width can produce a virtual sextupole. Moreover, the remanent field pattern is frozen in at high field where the flux lines leading to the pole edges are shorter than those leading to the centre. The remanent magnetomotive force

$$\int H_c d\ell$$

is weaker at the pole edges, and the field tends to sag into a parabolic or sextupole configuration. This too produces a sextupole.

These three sources of sextupole error are the principle non-linearities in a large machine like the SPS. Note that these sextupole fields have no skew component. However, before launching into nonlinearities let us examine a simple linear resonance.

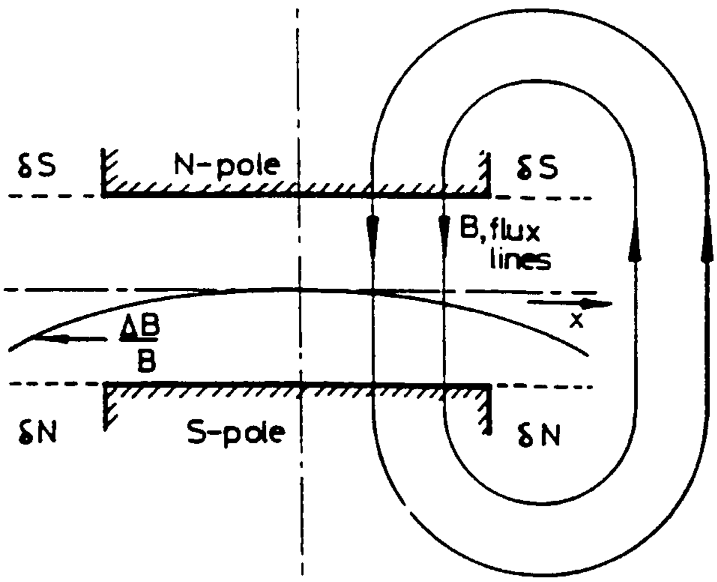

Fig. 3 The field in a simple dipole. The δN and δS poles superimposed on the magnet poles give the effect of cutting off the poles to a finite width.

3. SECOND-ORDER RESONANCE

A small elementary quadrupole of strength $\delta(Kl)$ is located close to an F quadrupole where $\beta_H = \hat{\beta}$. Suppose a proton describes a circular trajectory of radius $a = \sqrt{\varepsilon\beta}$ and encounters the quadrupole at phase:

$$Q\varphi(s) = Q\theta \ ,$$

where θ is the azimuth which corresponds exactly to φ at the quadrupoles of a FODO lattice.

The first step is to write down the unperturbed displacement at the small quadrupole:

$$x = a \cos Q\theta \ . \tag{5}$$

It receives a divergence kick (Fig. 4):

$$\Delta x' = \Delta(B\ell) / B\rho = \Delta(K\ell)x / B\rho \ . \tag{6}$$

The small change in $\hat{\beta}\Delta x'$,

$$\Delta p = \hat{\beta}\Delta x' \ , \tag{7}$$

perturbs the amplitude, a, by

$$\Delta a = \Delta p \ \sin Q\theta \ .$$

Even more significantly there is a small phase advance (Fig. 4):

$$2\pi\Delta Q = \frac{\Delta p}{a}\cos Q\theta \ . \tag{8}$$

By successive substitution of Eqs. (7), (6). and (5), we get

$$2\pi\Delta Q = \hat{\beta}\frac{\Delta(\ell K)}{(B\rho)} \ \cos^2 Q\theta \ . \tag{9}$$

Over one turn the Q changes from the unperturbed Q by

$$\Delta Q = \frac{\hat{\beta}\Delta(\ell K)}{4\pi(B\rho)}(\cos \ 2Q\theta + 1) \ . \tag{10}$$

On the average this shifts Q by

$$\Delta Q = \frac{\hat{\beta}\Delta(\ell K)}{4\pi(B\rho)} \ . \tag{11}$$

Similarly the change in amplitude, a, is on average:

$$\frac{\Delta a}{a} \approx 2\pi\Delta Q \ .$$

The first term, however, tells us that, as the phase $Q\theta$ on which the proton meets the quadrupole changes on each turn by 2π x (fractional part of Q), the Q-value for each turn oscillates and may lie anywhere in a band

$$\delta Q = \frac{\hat{\beta}\Delta(\ell K)}{4\pi(B\rho)}$$

about the mean value.

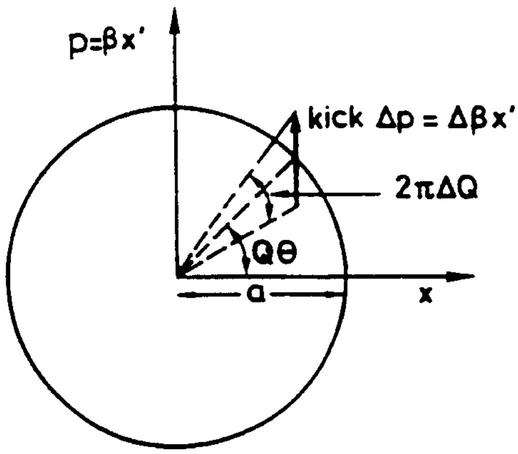

Fig. 4 Circle diagram shows effect of kick δpat phase $Q\theta$ advancing phase by $2\pi\Delta Q = (\Delta p \cos Q\theta)/a$

Suppose this band includes a half-integer Q-value. Eventually, on a particular turn, each proton will have exactly this half-integer Q-value ($Q = p/2$).

Because the first term in Eq. (10) is cos $2Q\theta$, the amplitude increases by $2\pi\Delta Q$ on the next and all subsequent turns. The proton has been perturbed by the $\Delta(Kl)$ error to a Q-value where it "locks on" to a half-integer stopband. Once there, the proton repeats its motion every two turns, and the small amplitude increase from the perturbation Δa builds up coherently and extracts the beam from the machine.

We can visualize this in another way by saying that the half-integer line in the Q diagram,

$$2Q = p \quad (p = \text{integer}) ,$$

has a finite width $\pm Q$ with respect to the unperturbed Q of the proton. Any proton whose unperturbed Q lies in this *stopband width* locks into resonance and is lost (Fig. 5).

In practice each quadrupole in the lattice of a real machine has a small field error. The $\Delta(lK)$'s are chosen from a random distribution with an r.m.s. value $\Delta(lK)$rms. If the N focusing quadrupoles at $\hat{\beta}$ have their principal effect, we can see that the r.m.s. expectation value for δQ is, from Eq. (11),

$$\langle \delta Q \rangle_{rms} = \sqrt{\frac{N}{2}}\frac{\hat{\beta}\Delta(K\ell)_{rms}}{4\pi B\rho} .$$

The factor √2 comes from integrating over the random phase distribution. The statistical treatment is similar to that used for estimating closed orbit distortion.

Now let us use some Fourier analysis to see which particular azimuthal harmonic of the $\delta(K$l) pattern drives the stopband. Working in normalized strength $k = \Delta K/(B\rho)$ we analyse the function $\delta(\beta k)$ into its Fourier harmonics with

$$\delta\beta k(s) = \sum \hat{\beta} k_p \cos(p\theta + \lambda) \qquad (12)$$

and

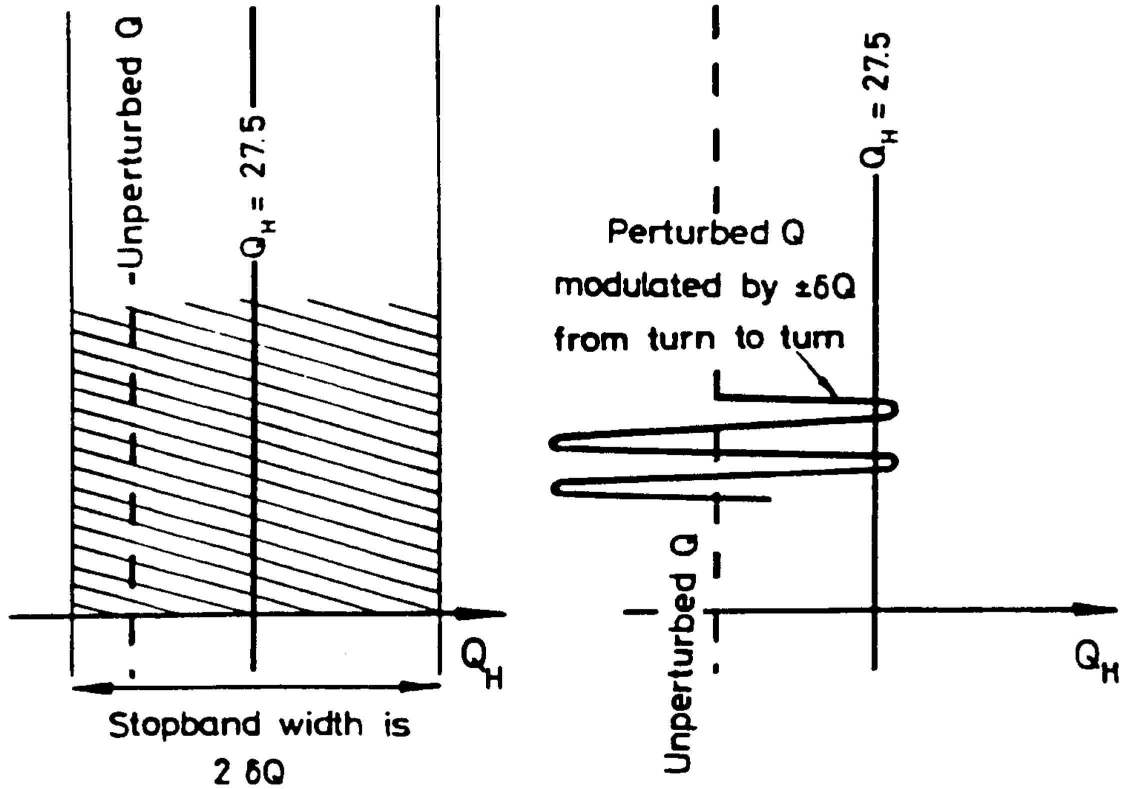

Fig. 5 Alternative diagrams showing perturbed Q and a stopband

$$\hat{\beta k}_p = \frac{1}{\pi R}\int_0^{2\pi} ds\,\delta[\beta k(s)]\cos(p\theta + \lambda) \ .$$

In general all harmonics i.e. all values of p, have equal expectation values in the random pattern of errors. We substitute the p^{th} term in Eq. (12) into Eq. (6) and work through the steps to obtain a new form for Eq. (10), namely:

$$2\pi\Delta Q = \int \frac{\hat{\beta k}_p}{2}\cos(p\theta + \lambda)\{\cos\, 2Q\theta + 1\}ds \ .$$

The integration can be simplified by writing $ds = Rd\theta$:

$$\Delta Q = \frac{\hat{\beta k}_p R}{4\pi}\int_0^{2\pi}\cos\, 2Q\theta\, \cos(p\theta + \lambda)d\theta \ .$$

The integral is only finite over many betatron oscillations when the resonant condition is fulfilled:

$$2Q = p \ .$$

We have revealed the link between the azimuthal frequency p in the pattern of quadrupole errors and the $2Q = p$ condition which describes the stopband. For example, close to Q = 27.6 in the SPS lies the half-integer stopband $2Q$ = 55. The azimuthal Fourier component which drives this is p = 55. Similarly, a pattern of correction quadrupoles, powered in a pattern of currents which follows the function

$$i = i_0 \ \sin\left(55\theta + \lambda\right) \ ,$$

can be used to compensate the stopband by matching i_0 and λ empirically to the amplitude of the driving term in the error pattern.

This has been used at the SPS, and in other machines powering sets of harmonic correction quadrupoles, each with its own power supply. We look for a sudden beam loss due to a strong stopband at some point in the cycle where Q' and $\Delta p/p$ are large and gradient errors important. This loss will appear as a downward step in the beam current transformer signal. We then deliberately make Q sit on the stopband at that point to enhance the step and alter the phase and amplitude of the azimuthal current patterns of the harmonic correctors to minimize the loss. We may have to do this at various points in the cycle with different phase and amplitude.

Two sets of such quadrupoles are used: one set near F lattice quadrupoles affecting mainly $2Q_H = 55$; the other set near D quadrupoles affecting $2Q_V = 55$.

4. THE THIRD-INTEGER RESONANCE

The third-integer stopbands are driven by sextupole field errors and are therefore non-linear. First imagine a single short sextupole of length l, near a horizontal maximum beta location. Its field is

$$\Delta B = \frac{d^2 B_z}{dx^2} x^2 = \frac{B''}{2} x^2 \ , \tag{13}$$

and it kicks a particle with betatron phase $Q\theta$ by

$$\Delta p = \frac{\beta \ell B''}{2B\rho} x^2 = \frac{\beta \ell B'' a^2}{2B\rho} \cos^2 Q\theta \tag{14}$$

inducing increments in phase and amplitude,

$$\frac{\Delta a}{a} = \frac{\Delta p}{a} \sin Q\theta = \frac{\beta \ell B'' a}{2B\rho} \cos^2 Q\theta \ \sin Q\theta \tag{15}$$

$$\Delta\phi = \frac{\Delta p}{a} \cos \ Q\theta = \frac{\beta \ell B'' a}{2B\rho} \cos^3 Q\theta \tag{16}$$

$$= \frac{\beta \ell B'' a}{8B\rho} \left(\cos 3Q\theta + 3 \cos Q\theta\right) \ . \tag{17}$$

Suppose Q is close to a third integer, then the kicks on three successive turns appear as in Fig. 6. The second term in Eq. (17) averages to zero over three turns and we are left with a phase shift:

$$2\pi\Delta Q = \Delta\phi = \frac{\beta \ell B'' a \ \cos 3Q\theta}{8\mathrm{B}\rho} \ . \tag{18}$$

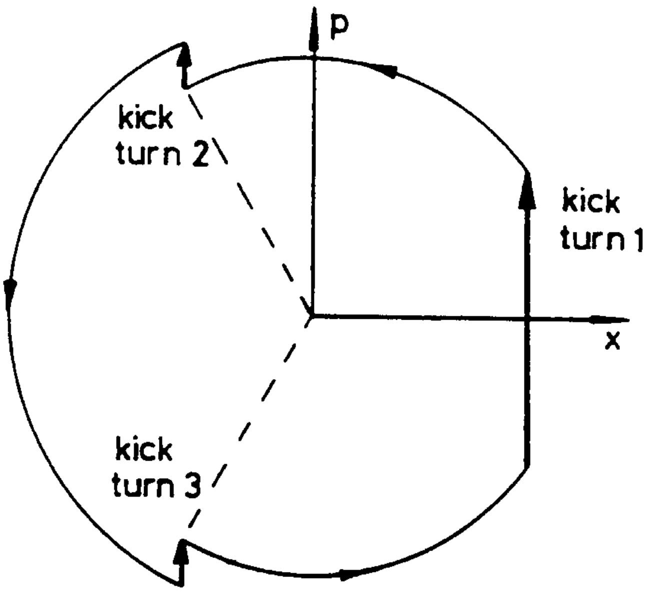

Fig. 6 Phase-space trajectory on a 3rd-order resonance

We can again guess how resonances arise. Close to $Q = p/3$, where p is an integer, $\cos 3Q\theta$ varies slowly, wandering within a band about the unperturbed Q_0 as in Fig. 5:

$$Q_0 - \frac{\beta \ell B'' a}{16\pi B\rho} < Q < Q_0 + \frac{\beta \ell B'' a}{16\pi B\rho} \ . \tag{19}$$

As in the case of the half-integer resonance this is the stopband width but in reality is a perturbation in the motion of the particle itself.

We can write the expression for amplitude perturbation

$$\frac{\Delta a}{a} = \frac{\beta \ell B'' a}{8B\rho} \sin 3Q\theta \ . \tag{20}$$

Suppose the third integer Q-value is somewhere in the band. Then, after a sufficient number of turns, the perturbed Q of the machine will be modulated to coincide with $3p$. On each subsequent revolution this increment in amplitude builds up until the particle is lost. Growth is rapid and the modulation of Q away from the resonant line is comparatively slow.

Looking back at the expressions, we find that the resonant condition, $3Q$ = integer, arises because of the $\cos^3 Q\theta$ term in Eq. (16), which in turn stems from the x^2 dependence of the sextupole field. This reveals the link between the order of the multipole and that of the resonance.

We see that the a^2 in Eq. (14) leads to a linear dependence of width upon amplitude. This term was a^1 in the case of the half integer resonance which led to a width which was independent of amplitude and will become a^3 in the case of a fourth-order resonance giving a parabolic dependence of width upon amplitude.

It is also worth noting that the second term in Eq. (17), which we can ignore when away from an integer Q-value, suggests that sextupoles can drive integer stopbands as well as third integers. Inspection of the expansion of $\cos^n\theta$ will suggest the resonances which other multipoles are capable of driving.

Returning to the third-order stopbands, we note that both stopband width and growth rate are amplitude-dependent. If Q_0 is a distance ΔQ from the third integer resonance, particles with amplitudes less than

$$a < \frac{16\pi(B\rho)\Delta Q}{\beta\ell B''} \tag{21}$$

will never reach a one third integer Q and are in a central region of stability. Replacing the inequality by an equality, we obtain the amplitude of the metastable fixed points in phase space where there is resonant condition but infinitely slow growth (Fig. 7).

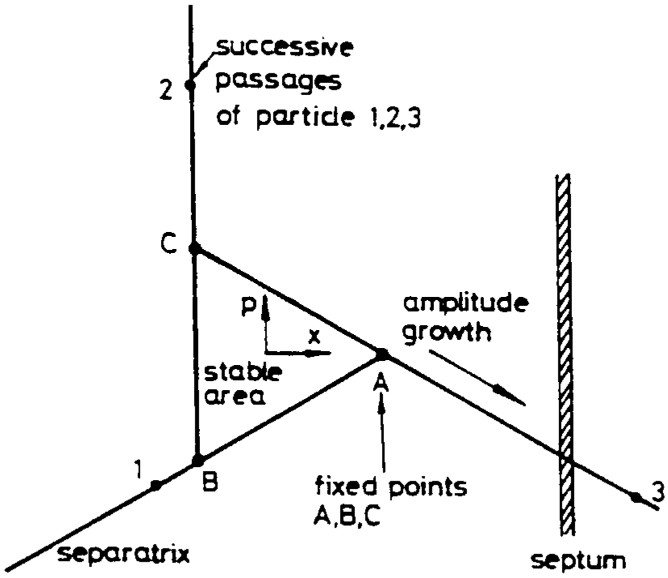

Fig. 7 Third-order separatrix

The symmetry of the circle diagram suggests there are three fixed points at $\theta = 0$, $2\pi/3$, and $4\pi/3$. For a resonance of order, n, there will be n such points.

The fixed points are joined by a separatrix, which is the bound of stable motion. A more rigorous theory, which takes into account the perturbation in amplitude, would tell us that the separatrix is triangular in shape with three arms to which particles cling on their way out of the machine.

We have seen how a single sextupole can drive the resonance. Suppose now we have an azimuthal distribution which can be expressed as a Fourier series:

$$B''(\theta) = \sum B_p'' \cos p\theta \ . \tag{22}$$

Then

$$\Delta\phi = \sum_p \int \frac{\beta B_p''}{8B\rho} \cos 3Q\theta \cos p\theta d\theta \ . \tag{23}$$

This integral is large and finite if

$$p = 3Q \ . \tag{24}$$

As in the earlier case of the second-order resonances this reveals why it is a particular harmonic in the azimuthal distribution which drives the stopband. It is not just the Fourier spectrum of $B''(\theta)$ but of $\beta B''(\theta)$ which is important in this context. Periodicities in the lattice and in the multipole pattern can thus mix to drive resonances.

This is particularly important since some multipole fields, like the remanent field pattern of dipole magnets, are inevitably distributed in a systematic pattern around the ring. This pattern is rich in the harmonics of S, the superperiodicity. Even when this is not the case and errors are evenly distributed, any modulation of beta which follows the pattern of insertions can give rise to systematic driving terms. It is an excellent working rule to keep any systematic resonance, i.e.

$$\ell Q_H + mQ_V = S \ (\text{superperiod number}) \times \text{integer} = p \tag{25}$$

out of the half integer square in which Q is situated. This is often not easy in practice.

As in the second-order case, the third-order stopbands can be compensated with sets of multipoles powered individually to generate a particular Fourier component in their azimuthal distributions. The above equation defines four numerical relations between Q_H and Q_V which are resonant. The keen student can verify this with an extension to the mathematics of the previous section. He will find that two of the lines are sensitive to errors of a sextupole configuration with poles at the top and bottom, the other two to sextupoles with poles symmetrical about the median plane (Fig. 2). By permuting these two kinds of sextupoles with the two types of location, we can attack the four lines more or less orthogonally.

5. GENERAL NUMEROLOGY OF RESONANCES

We have seen how the Q-value at which the resonance occurs is directly related to a frequency in the azimuthal pattern of variation of multipole strength. We can now generalise this.

Suppose the azimuthal pattern of a multipole of order n can be Fourier analysed:

$$B^{(n-1)}(\theta) = \sum_p B_p^{(n-1)} \cos p\theta \ , \tag{26}$$

where θ is an azimuthal variable, range 0 to 2π. We shall show that if the resonance is in one plane only, a particular component, $p = nQ$, of this Fourier series, drives it. For example, the 83rd azimuthal harmonic of sextupole ($n = 3$) drives the third-order resonance at $Q = 27.66$. The more general expression is

$$\ell Q_H + mQ_V = p \tag{27}$$

$$|\ell| + |m| = n \ (\text{an integer}) \ . \tag{28}$$

Each n-value defines a set of lines in Fig. 1, four for third-order resonances, five for fourth-order, etc. Each line corresponds to a different homogeneous term in the multipole Cartesian expansion (Table 1). Some are excited by regular multipoles, others by skew multipoles.

6. SLOW EXTRACTION USING THE THIRD-ORDER RESONANCE

So far we have thought of resonances as a disease to be avoided, yet there is at least one useful function that they can perform.

We have seen that a third-order stopband extracts particles above a certain amplitude, the amplitude of the unstable fixed points which define a separatrix between stability and instability

(Fig. 7). The dimensions of the separatrix, characterized by a are determined by ΔQ, the difference between the unperturbed Q and the stopband. As one approaches the third integer by, say, increasing the focusing strength of the lattice quadrupoles, ΔQ shrinks, the unstable amplitude, a, becomes smaller and particles are squeezed out along the three arms of the separatrix. If we make ΔQ shrink to zero over a period of a few hundred milliseconds, we can produce a rather slow spill extraction.

At first sight we might expect only one third of the particles to migrate to positive x-values since there are three separatrices, but it should be remembered that a particle jumps from one arm to the next each turn, finally jumping the extraction septum on the turn when its displacement is largest. The septum is a thin walled deflecting magnet at the edge of the aperture.

The growth increases rapidly as particles progress along the unstable separatrix, and if the stable area is small compared with the distance between beam and septum, the probability of a particle striking the septum rather than jumping over it is small. It clearly helps to have a thin septum. The SPS it is a comb of wires forming a plate of an electrostatic deflector.

Magnet or quadrupole ripple can cause an uneven spill, making the Q approach the third integer in a series of jerks thus modulating the rate at which particles emerge. A spread in momentum amongst the particles can help, however, since if the chromaticity is finite, we will have swept through a larger range of Q-values before all separatrices for all momenta have shrunk to zero. The larger Q change reduces the sensitivity to magnet ripple.

7. LANDAU DAMPING WITH OCTUPOLES

Another beneficial effect of multipoles is the use of octupoles to damp coherent transverse instabilities due to the beam's own electromagnetic field.

For a transverse instability to be dangerous, the growth time must win over other mechanisms which tend to destroy the coherent pattern and damp out the motion. One such damping mechanism is the Q-spread in the beam. Coherent oscillations decay, or become dephased, in a number of betatron oscillations comparable to $1/\Delta Q$, where ΔQ is the Q-spread in the beam. This corresponds to a damping time, expressed in terms of the revolution frequency, $\omega_0/2\pi$:

$$\tau_d = \frac{2\pi}{\omega_0 \Delta Q} \ , \tag{29}$$

which is just the inverse of the spread in frequencies of the oscillators involved, i.e. the protons. The threshold for the growth of the instability is exceeded when τ_g (which increases with intensity) exceeds τ_d

$$\tau_g = \frac{2\pi}{\omega_0 \Delta Q} \ . \tag{30}$$

This is a very general argument which affects all instability problems involving oscillators and is an example of *Landau damping.* Thinking of it another way, we can say that the instability never gets a chance to grow if the oscillators cannot be persuaded to act collectively for a time τ_g. If they have a frequency spread Δf, the time for which they can act concertedly is just $1/\Delta f$.

Unfortunately, in our quest for a small ΔQ to avoid lines in the Q diagram by correcting chromaticity, improvements in single particle dynamics can lower the threshold intensity for the instability. A pure machine is infinitely unstable. In practice, at the SPS this happens at about 5×10^{12} particles per pulse if ΔQ is less than 0.02 and τ_g about 1 msec. Suddenly the beam begins to snake under the influence of the resistive wall instability. A large fraction of the beam is lost before stability is restored.

The first remedy is to increase ΔQ. Landau damping octupoles are installed for this purpose in the SPS. Octupoles produce an amplitude Q-dependence which is thought to be more effective than the momentum-dependent Q-spread produced by sextupoles. Each particle changes in momentum during a synchrotron oscillation, and in a time comparable to τ_g all particles have the same mean momentum. Sextupoles do not spread the mean Q of the particles. Octupoles, producing an amplitude Q-dependence, do.

The circle diagram can be used to calculate the effect of an octupole which gives a kick:

$$\Delta p = \beta \frac{\Delta(B\ell)}{B\rho} = \frac{\beta \ell B'''}{3!(B\rho)} a^3 \cos^3 Q\theta \ . \tag{31}$$

The change in phase is

$$2\pi\Delta p = \Delta\phi = \frac{\beta \ell B''' a^2 \ \cos^4 Q\theta}{6(B\rho)} \ , \tag{32}$$

which averages to

$$\Delta Q = \frac{\beta \ell B''' \beta a^2}{32\pi B\rho} \ . \tag{33}$$

Of course if the octupoles are placed around the ring they can excite fourth-order resonances. A good rule is to have as many of them as possible and to distribute them at equal intervals of betatron phase. If there are S octupoles thus distributed their Fourier harmonics are S, $2S$, etc. and they can only excite structure resonances near Q values:

$$4Q = S \times \text{ an integer } .$$

Although these systematic resonances are very strong it should not be difficult to choose S so that Q is not in the same integer square as one of the values of $nS/4$.

* * *

FURTHER READING

G. Guignard, Effets des Champs Magnetique Perturbateurs d'un Synchrotron - CERN 70-24 (1970), p. 67-lOS.

M.H. Blewett (Editor), Theoretical Aspects of the Behaviour of Beams in Accelerators and Storage Rings - CERN 77-13 (1977), p. 111-138.

G. Guignard, A General Treatment of Resonances in Accelerators, CERN 78-11 (1978).